CrossMark

Characterization of temperature-dependent tensile and flexural rigidities of a cross-ply thermoplastic lamina with implementation into a forming model

Lisa M. Dangora[1] · Cynthia Mitchell[1] · Kari D. White[1] ·
James A. Sherwood[1] · Jason C. Parker[2]

Abstract This paper discusses the characterization of temperature-dependent tensile and flexural rigidities for Dyneema® HB80, a cross-ply thermoplastic lamina. The low coefficient of friction of this material posed a challenge to securing specimens during tensile testing. Therefore, modification to the standard gripping method was implemented to facilitate the collection of meaningful test data. Furthermore, a long gauge length was selected to moderate the influence of slippage on the measure of the elastic modulus. A new experimental setup is presented to characterize the bending behavior at elevated-temperature conditions based on the vertical cantilever method. The material properties derived from the test data were implemented in a finite element model of the cross-ply lamina. The finite element model is generated using a hybrid discrete mesoscopic approach, and deep-draw forming of the material is simulated to investigate its formability. Simulation results are compared with an experimental forming trial to demonstrate the capabilities of the model to predict the development of out-of-plane waves during preform manufacturing.

✉ James A. Sherwood
james_sherwood@uml.edu

1 Department of Mechanical Engineering, University of Massachusetts
Lowell, 1 University Ave., Lowell, MA 01854, USA

2 US Army Natick Soldier Research, Development & Engineering
Center, 15 Kansas St., Natick, MA 01760, USA

Introduction

Composite materials are experiencing rapid market growth and becoming increasingly popular across a variety of industries including aerospace, automotive, construction, marine, and wind energy [1]. However, a large percentage of the potential market is lost when designers are apprehensive about the predictability of composite performance. For example, consider how continuous-fiber-reinforced composites are prone to wrinkling. Such defects are a consequence of the combination of the mechanical behavior of the materials and the manufacturing processing conditions, and these defects result in compromised load paths and stress concentrations that can lead to catastrophic and premature failures [2]. Furthermore, uncertainties in both material behavior and processing conditions can often result in overdesigned parts, unnecessarily increasing weight and cost. As such, many designers remain complacent using conventional bulk materials (e.g., metals, ceramics, and polymers) with predictable mechanical behaviors. Therefore, growth of the composite market will continue to be slow until credible software tools that can be used to explore the relationship between material formability and design constraints become available and widely used.

Because wrinkling of the composite reinforcement can result in premature failure, it is important that the manufacturing process be designed to mitigate formation of such unwanted shape distortions. As a result, the processing parameters will be driven by the forming limits of the material and the relative complexity of the part geometry. Unfortunately, the processing conditions that create an environment which is conducive for wrinkle development are not always known before the development phase. Consequently, correction of adverse product features is often accomplished with a design-build-test regimen, which can be costly, wasteful, and time

🖄 Springer

consuming. A simulation tool that could perform the design-build-test activity in a virtual setting would provide a cost and time efficient solution to product development and process design.

While there are various commercial software applications available to perform draping simulations (e.g., Fibersim and CATIA), the "fishnet" algorithms [3–7] used in these design tools are limited to purely kinematic analyses to predict deformation of the blank as it conforms to tool geometry. These geometric approaches are fast and efficient, but they do not account for the mechanical behavior of the fabric nor do they consider the boundary conditions of the forming process (e.g. any in-plane stress induced by a blank holder). As a result, these "fishnet" methods are unable to predict if and where in-plane waviness and out-of-plane wrinkling may occur during the forming of continuous-fiber reinforcements. Therefore, a mechanical analysis that includes the material behavior is necessary to predict the locations and magnitudes of defects that may develop during manufacture.

Using a discrete mesoscopic finite element model, information regarding thickness changes, fiber orientations, stresses and strains can be mapped over the preform surface and monitored throughout the forming process [8]. With a complete set of material properties for describing the material behavior, the simulation tool is able to identify potential defects (e.g., in-plane waves, out-of-plane wrinkles, fiber tearing) that arise during manufacture and compromise the part performance. Results of the finite element analysis (FEA) can therefore be used to guide the selection of processing parameters (e.g., tool velocity, forming temperature, binder pressure, material selection, ply geometry, and binder size) such that the resulting preform satisfies the design constraints (e.g., fiber orientations, uniform thickness and low seam density).

In the current paper, the shear, flexural, and tensile rigidities of Dyneema® HB80 are characterized at the lamina's forming temperature for input into the material model of a finite element simulation. The combined effect of these mechanical properties translates into a realistic depiction of the progressive composite deformation during the manufacture of a composite preform using this material system. The major novelty of this work is that it serves to extend the capabilities of FEA models to accommodate temperature-dependent material behavior of fiber-reinforced thermoplastics. The credibility of the beam/shell approach for the modeling of the forming of Dyneema® HB80 sheets at elevated temperature is demonstrated through (1) the characterization of material properties necessary for input into a finite element model of the forming process and (2) the simulation of near-net-shape preforming. A qualitative comparison between out-of-plane wrinkles resulting in experimentally-formed parts and model predictions of the composite system is presented and discussed.

Modeling approach

The multi-scale nature of fibrous materials poses challenges to analyzing the true behavior of textile composites [9–11]. Macroscopic models are often too homogenized to capture the intrinsic fabric response while micromechanical analyses require significant computational capacity to simulate forming of a full-scale part. As such, the modeling performed for this research is accomplished at the mesoscopic scale using a discrete approach developed by Jauffrès et al. [3] employing a hypoelastic element description with an explicit formulation.

The textile constituents are modeled using conventional elements available in commercial finite element software. Linear beam elements incorporate the tensile and flexural properties of the tows, while shell elements define the shear response of the fabric. For example, a cross-ply is discretized into a mixed-mesh grid where the unit cell consists of four beam elements and one shell element (Fig. 1). The shell element has no tensile properties and only possesses in-plane shear stiffness that varies with the degree of shear. The two horizontal beam elements are defined using properties of the 0° fibers, and the two vertical beam elements are defined using properties of the 90° fibers. A single node is used to connect the intersecting beam elements at each of the shell corners. This joining of the beams assumes a "no slip" condition between 0° and 90° layers which has been demonstrated to be an acceptable assumption [12, 13].

This modeling technique has been applied to a variety of textile architectures including woven, unidirectional, and non-crimp fabrics [14–16]. For this research, analyses are performed using the explicit solver in Abaqus which offers capabilities for analyzing large, nonlinear, quasi-static problems, such as deep-drawing. Furthermore, Abaqus/Explicit implements robust contact algorithms without the need for additional degrees of freedom, and it can resolve solution discontinuities such as buckling or wrinkling. The implicit analysis by Abaqus/Standard is less practical for solving this class of complicated forming processes that have many contact constraints
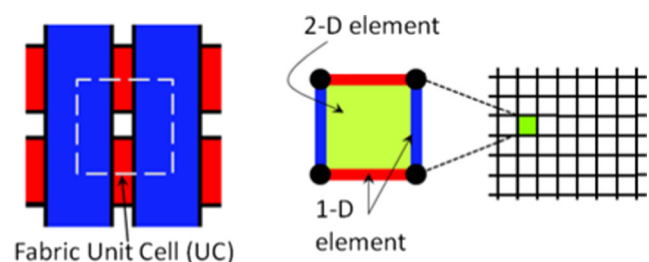
Fig. 1 A representative unit cell for the finite element discretization of a textile reinforcement
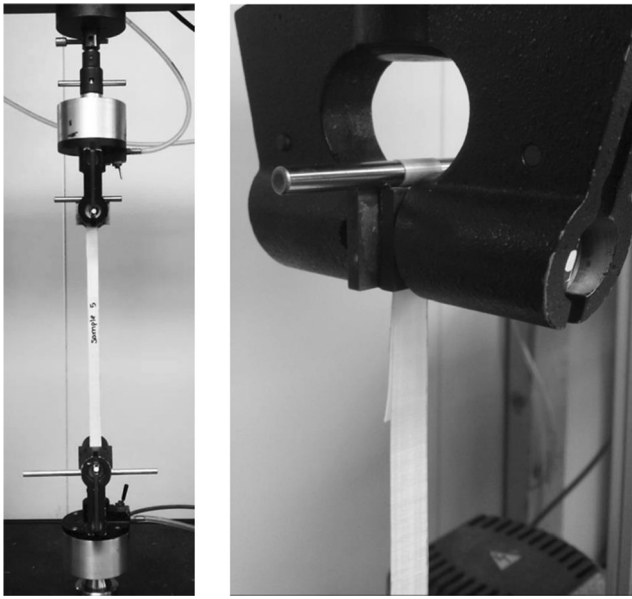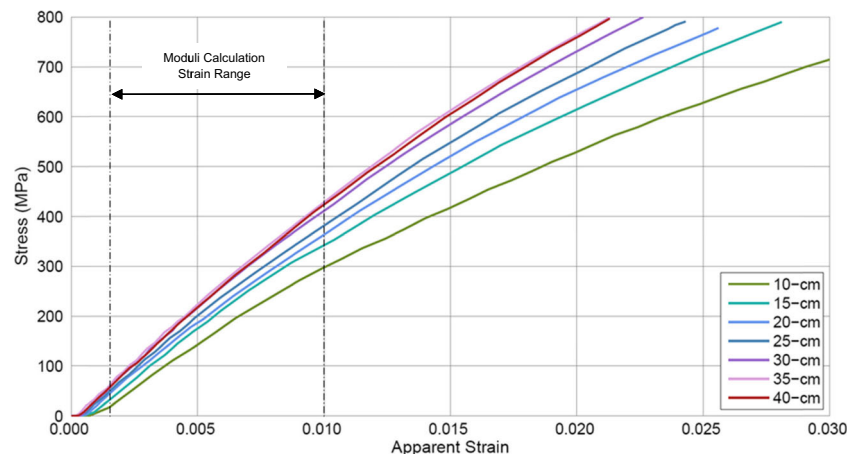
Fig. 2 Experimental setup for the measure of apparent tensile modulus using a modified gripping method to secure the sample by wrapping it around an external pin

Gauge length (cm)	Apparent modulus (GPa)
10	33
15	37
20	38
25	40
30	43
35	44
40	44

Table 1 Apparent modulus as a function of gauge length

and frictional effects [17]. User-defined material subroutines are linked to the Abaqus solver to govern beam and shell behavior [3]. The accuracy of the simulation is dependent on the quality of material constants derived from characterization tests that describe the fabric in bending [18, 19], tension [20, 21], and shear [22–25], and on the ply/tool and ply/ply interfacial friction [26].

Material characterization

While the material characterization methodologies that are described in this paper are applicable to a wide range of fiber-reinforced material systems, the specific material considered in this research is Dyneema® HB80, a thermoplastic cross-ply

containing four unidirectional layers oriented in a $(0/90)_2$ initial fiber configuration. Ultrahigh molecular weight polyethylene (UHMWPE) fibers and a thermoplastic polyurethane (TPU) based matrix comprise the highly fibrous lamina where the TPU content ranges between 15% and 20% by weight (17.9% and 23.6% by volume). Approximately 10 fibers contribute to the ply thickness of 0.148 mm, and the sheets have an average areal density of 145 g/m^2 [27–29]. Due to the polymeric nature of the constituent materials, the mechanical behavior of the composite system will exhibit temperature dependence and must therefore be characterized over the range of possible forming temperatures. A detailed description for the novel methodology used for the characterization of the shear behavior is given in Dangora *et al.* [25]. The current paper presents the complementary characterization of the tensile and flexural rigidities.

Tensile testing

The standard test method for breaking force and elongation of textile fabrics (ASTM-D5035) was used to measure the apparent elastic modulus of Dyneema® HB80 as a function of temperature [21]. These tensile experiments were executed on an Instron 4464 universal testing machine using pneumatic grips

Fig. 3 Tensile results for various gauge lengths tested under ambient conditions. Note that the vertical dashed lines indicate the range over which the moduli were calculated
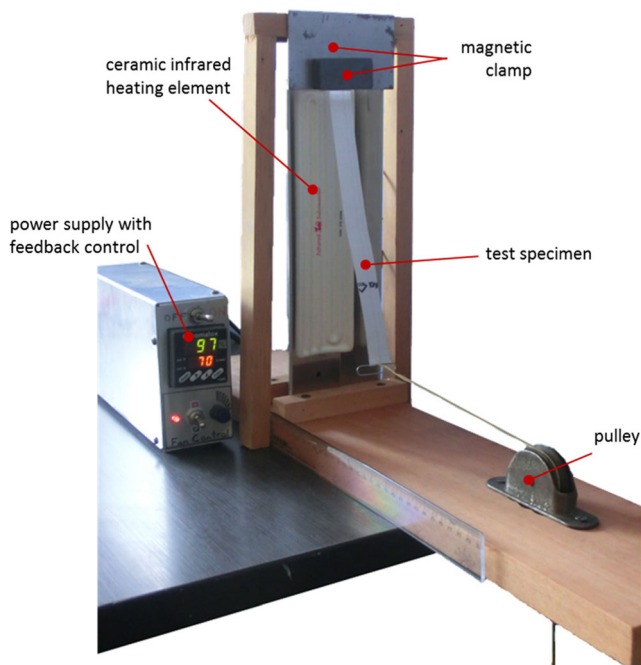
Fig. 4 Experimental setup for evaluation of bending stiffness at elevated temperatures based on the vertical cantilever method defined in [19]

with flat-faced jaws at a pressure of 620 kPa and a crosshead displacement rate of 1.7 mm·s^{-1}. Due to a 2-kN limit on the load cell, the sample geometry was modified from ASTM-D5035 specifications to have a 13-mm width. This smaller section allowed the specimens to be tested to failure at the forming temperatures of interest without damaging the load cell. Use of an extensometer was avoided to prevent damage of the polymer fibers during testing; therefore, the strain measurements were evaluated based on the displacement of the clamps. Where test setup compliances and sample slip were inherent to this measure, the true fiber elongation was not able to be recorded; instead an "apparent" modulus was reported in accordance with the ASTM-D5035 documentation [21, 30, 31]. Statistically insignificant variance in modulus was
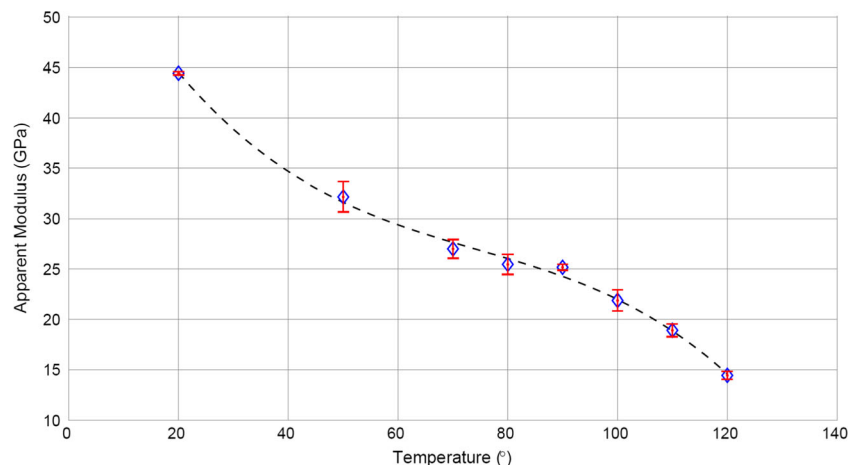
observed between samples tested under the same conditions for the 0° and 90° degree orientations. Therefore, the experimental schedule was only conducted in the 0° direction.

The tested material had an extremely low coefficient of friction [32], making it difficult to secure the specimens [29]. Therefore, to improve gripping of the sample and to minimize slippage, 6.35-mm diameter steel pins were used outside the jaws. The specimens were mounted such that the samples came through the grips, around the pin, and then back through the grips (see Fig. 2). The faces in contact with the jaw surfaces had fibers oriented in the loaded direction, while the faces in contact with the pins had fibers oriented in the cross direction. Tabbing was also investigated, but the modified gripping method in Fig. 2 was found to be most effective.

To observe the effects of slippage, the influence of gauge length on tensile response was investigated [30]. This study was conducted at room temperature for samples having gauge lengths ranging from 10 to 40 cm in 5-cm increments. It was expected that the influence of slippage would be less prominent for larger gauge lengths. This hypothesis was confirmed by the data shown in Fig. 3. As the sample length increased, the curves converged to a single solution. The slopes of stress-strain curves for the longest gauge lengths converged to the expected modulus, which was approximated using the Rule of Mixtures [33]. The vertical lines in Fig. 3 depict the range of strain used in completing the linear regression for slope calculation.

The Rule of Mixtures is derived from a constant-strain analysis, and it can be used to estimate the upper-bound of the modulus for a composite system. The value is approximated from contributions of the constituent material properties such that the composite modulus in the 0° direction, $E_c^{0°}$, is given by

$$E_c^{0°} = \phi_m E_m + \phi_f^{0°} E_{1f}^{0°} + \phi_f^{90°} E_{2f}^{90°} \tag{1}$$

Fig. 5 The apparent tensile modulus of Dyneema® HB80 follows a third-order polynomial (denoted by the dashed line) when plotted as a function of temperature. Note that the modulus was consistent for both 0° and 90° directions, and the error bars shown denote standard deviation over five samples

Fig. 6 Representative tensile data for Dyneema® HB80 tested at various temperatures. Note that the samples at 20°C and 50°C were not tested to failure due to max load limitations of the load cell
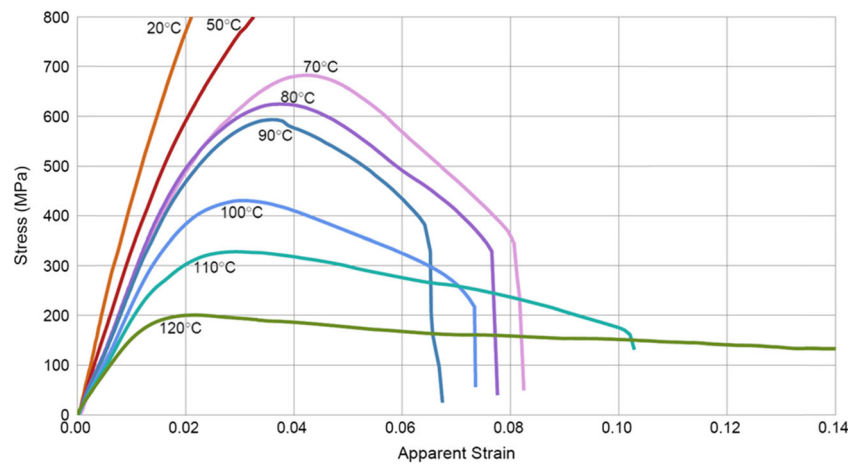
where ϕ is the volume fraction, E is the elastic modulus, and the subscripts m and f denote properties of the matrix and fiber, respectively. The notation E_1 refers to the longitudinal modulus (i.e., along the fiber axis) and E_2 indicates the transverse modulus (i.e., orthogonal to the fiber alignment). Highly-oriented polymer filaments, like the Dyneema® fibers, have extremely low degrees of transverse bonding due to the weak hydrogen bonds and Van der Waals attractions that govern interaction between adjacent chains [28]. Therefore, the reinforcing fibers in the composite lamina provide essentially no transverse stiffness (i.e., $E_2 \approx 0$). As such, when the material is tested in the 0° direction, the contribution from the 90° fibers is effectively negligible. Because the matrix modulus is much, much less than the fiber longitudinal modulus [29], Eq. 1 reduces to

$$E_c^{0°} = \phi_f^{0°} E_{1f}^{0°} \qquad (2)$$

and the stiffness of the composite lamina is dominated by the properties of the 0° fibers. These fibers are reported to have a tensile modulus of approximately 116 GPa [34]. With the matrix content ranging from 17.9% to 23.6% by volume, the fibers comprise 76.4% to 82.1% of the ply; specifically, the 0° fibers account for half of this fiber volume. Therefore, Eq. 2 suggests

that the lamina should have a modulus between 44 GPa and 48 GPa. As the experimental values converged to 44 GPa, the effect of slippage was assumed to be negligible for specimen lengths greater than or equal to 35 cm. A summary of the apparent moduli for these gauge lengths is provided in Table 1. Execution of the final measurements was conducted for a gauge length of 42 cm over an average of five samples.

Bend testing

Because the bending rigidity governs the shapes of wrinkles that form during textile draping and composite forming, it is important to represent this property accurately in the finite element model. Unlike conventional isotropic materials, the bending stiffness of fibrous materials is not directly related to the tensile modulus; it must therefore be measured through experimentation [10]. While there exists a standard test method for characterization of the bending rigidity [18], Lammens *et al.* demonstrated that use of the ASTM D1388 cantilever test results in measures with severe inaccuracies [35]. Furthermore, the ASTM documentation does not address materials exhibiting temperature-dependent behavior. Therefore, several experimental methods have been developed to measure flexural stiffness above ambient conditions [36–39].

Table 2 Summary of temperature-dependent tensile behavior for Dyneema® HB80

	Apparent modulus (GPa)			Tensile strength, UTS (MPa)			Strain at UTS (%)		
20°	44.4	±	0.2	*			*		
50°	32.2	±	1.5	*			*		
70°	27.0	±	0.9	669	±	26	3.98%	±	0.25%
80°	25.5	±	1.0	604	±	24	3.82%	±	0.29%
90°	25.2	±	0.3	592	±	11	3.90%	±	0.07%
100°	21.9	±	1.0	435	±	06	3.15%	±	0.08%
110°	18.9	±	0.6	310	±	14	2.74%	±	0.19%
120°	14.4	±	0.4	192	±	09	2.20%	±	0.10%

*Not tested to failure due to load-cell limitations

Fig. 7 Deflection of Dyneema® HB80 strips subject to the same loading at different temperatures
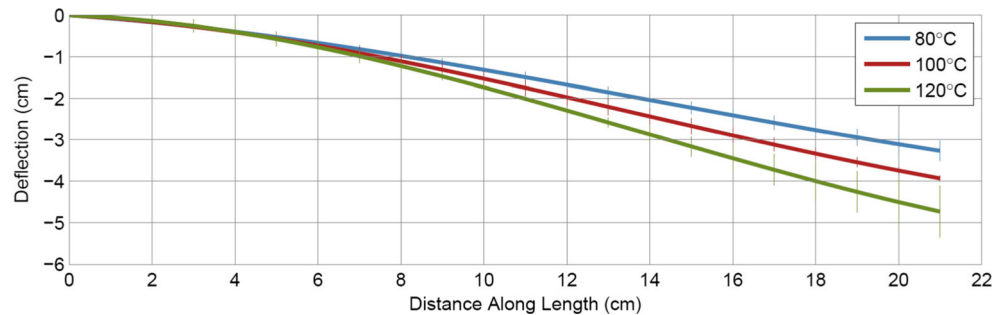
For the purpose of the research presented in this paper, the simple vertical cantilever test proposed in [19] was used. The experimental setup described in [19] was modified to accommodate characterization at elevated temperatures. The test fixture, shown in Fig. 4, heated the sample using radiation from a concentrated ceramic infrared (IR) element. A feedback control system with a Type-J thermocouple sensor was used to regulate the temperature of the ceramic elements. An additional Type-J thermocouple was added for monitoring the test-specimen temperature on the surface of the lamina away from the IR heating to ensure uniform through-thickness temperature. To enforce the cantilever boundary condition, a magnetic clamp was used. The ceramic block magnet had a stability temperature of 250°C and a maximum pull force of 60 N. Although the Dyneema® HB80 specimens were only 0.148-mm thick, a strong magnet was selected so the experimental setup could also be used for much thicker specimens in the future. The free end of the sample was displaced using a hanging mass on a string, redirected downward with a pulley. The test protocol followed the procedures outlined in [19] with a gauge length of 25 cm and specimen width of 20 mm. While the matrix deformation in bending was presumably governed by interlaminar shear, this property was not separately investigated. With the high fiber content, the response of the lamina in bending was largely dominated by the fiber mechanics; and as the sample length was significantly larger than the thickness, interlaminar shearing of the fibers was considered to be negligible.

Results and discussion

The material was tested for temperature-dependent tensile and flexural rigidities in accordance with the aforementioned procedures. The combination of these material properties, in conjunction with the shear behavior (previously characterized in Dangora *et al.* [25]), facilitated development of a forming model. Data collected from the characterization tests are presented in this section in addition to the results of a finite element deep-draw simulation.

Tensile testing

Tensile tests were performed on strips of Dyneema® HB80 for temperatures ranging from 70°C to 120°C, testing five specimens for each temperature. For reference, additional data were collected below the possible forming limits at ambient conditions and at 50°C. Note that no statistically-significant difference was observed between testing in the 0° and 90° directions subject to identical experimental conditions. Load-displacement data collected from the experiments were used to calculate the lamina's apparent modulus as a function of temperature (Fig. 5). The

Fig. 8 Moment-curvature relation for Dyneema® HB80 samples in bending at elevated temperature
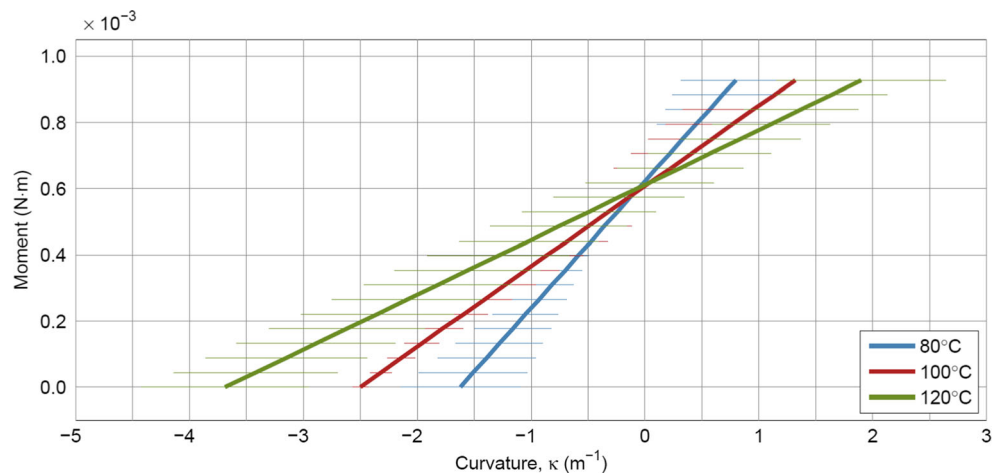
Table 3 Summary of flexural stiffness for Dyneema HB80 tested at elevated temperatures

Temperature (°C)	Bending rigidity (N·mm^2)
80°	380
100°	240
120°	170

resulting data were found to best follow a third-order polynomial over the range of temperatures studied. As was expected, increasing the temperature made the material more compliant. The addition of heat facilitated motion of the polymer chains, thereby reducing the stiffness. A representative data set was plotted for each of the test conditions (Fig. 6). To avoid damage to the 2-kN load cell, the ambient and 50°C samples were not tested to failure. The data trends indicated that, with an increase in temperature, there were an associated (1) decrease in modulus, (2) reduction in yield strength/strain, and (3) increase in ductility.

A summary of the apparent modulus and tensile strength for each temperature is presented in Table 2. Although values for ultimate tensile strength (UTS) and the corresponding strains were identified from the stress-strain curves over the possible forming temperatures, these data were not essential to the modeling efforts. Because plastic deformation was not incorporated into the finite element analysis, the only critical information obtained from tensile testing was the elastic modulus. Future modeling work could consider plastic deformation.

While the UTS may not have been considered in the analysis, these data could still be useful in post-processing. For example, the simulation results can be used to map color contours of stress and strain across the formed part; the analyst can use these outputs and the experimental strength values to identify potential areas of fiber damage. However, because the ultimate strength is known to be dependent on sample size, a Weibull modulus would need to be calculated if these properties were of concern [30].

Bend testing

Because there was not enough resolution in the bend testing data to differentiate data over a ± 10°C temperature variation, bend tests were performed at 80°C, 100°C, and 120°C. Softening of the material was apparent with the addition of heat. As the temperature was increased, the sample exhibited increased deflection under identical loading conditions (Fig. 7). Pictures were taken of the loaded samples and ImageJ, an open-source image analysis software, was used to measure discrete displacements. A third-order polynomial was fit to the data, and the curves shown in Fig. 7 are the respective fits for an average of three test samples. A detailed description of the methods used to interpret the data is given in Dangora *et al.* [19]. The curvature was approximated by taking the second derivative of the average deflection equation. Because the force used to displace the cantilever's free end was measured, the moment along the sample was known. This information was used to plot the moment as a function of curvature (Fig. 8). The bending stiffness was derived from the slope of the moment-curvature line, and these values are summarized in Table 3. Although the flexural-rigidity values remained on the same order of magnitude over the temperature range investigated, the temperature dependence is sufficiently significant to recommend using the temperature-based bending properties in the forming simulation.

Forming experiment and simulation

Hemisphere forming was performed using the experimental setup shown in Fig. 9a and described in detail by Dangora *et al.* in [40]. The fixture (consisting of a hemispherical punch, an open die, and a blank holder) was placed in an environmental chamber and mounted on a universal testing machine. A single sheet of Dyneema® HB80 was heated to a forming

Fig. 9 Hemisphere deep-draw (**a**) experimental setup and (**b**) associated configuration for FEA

(a)

(b)
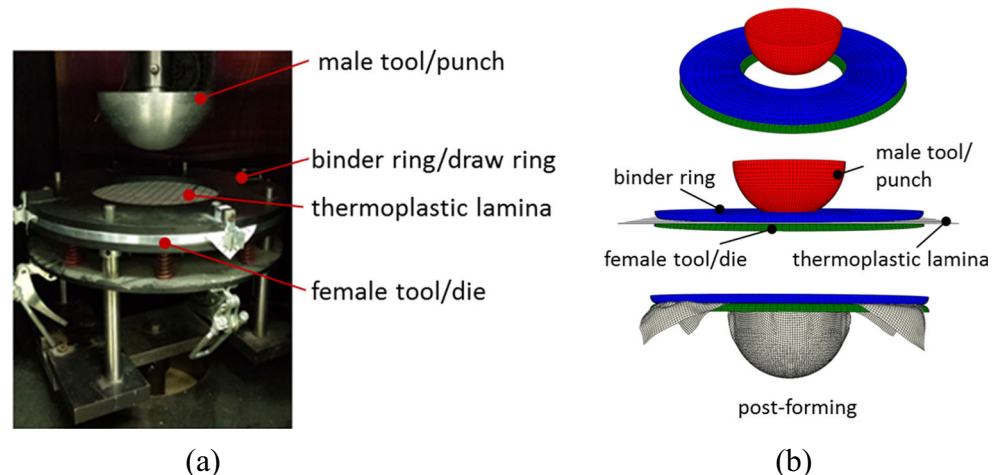
Table 4 Summary of material constants at 100°C for model input

Property	Value (MPa)
Tensile modulus	22,000
Compressive modulus	215
Shear stiffness* [25]	$23|\gamma|^4 - 55|\gamma|^3 + 48|\gamma|^2 - 17|\gamma| + 3$

*Note that γ is defined as the shear strain of the composite lamina

temperature of 100°C and drawn to the punch geometry. Approximately 3200 Pa of pressure was applied to the blank to supply in-plane tension as the sheet was drawn.

Similarly, a deep-draw forming simulation at 100°C was completed in Abaqus/Explicit using the configuration shown in Fig. 9b. A pressure of 6500 Pa was applied to the binder ring to hold the lamina between the ring and the die during the forming and a fabric-tool friction coefficient of 0.07. The tensile modulus and bending stiffness previously measured were used to calculate an effective compressive modulus (E_c) for implementation in the finite element model following the equation

$$B = E_t I \frac{4^{E_c/E_t}}{\left(\sqrt{E_c/E_t} + 1\right)^2} \qquad (3)$$

as developed by Dangora *et al.* [19], where B is the bending stiffness, E_t is the tensile modulus, and I is the area moment of inertia. The compressive modulus at 100°C was calculated to be 215 MPa and the bilinear modulus was implemented into the finite element model. Note that the lamina properties were assigned to the beam elements, not the fiber properties. The measurement methods of the temperature-dependent shear stiffness for the Dyneema® H80 are outlined in Dangora *et al.* [25]. A summary of the material constants used in the model are provided in Table 4.

The experimental and finite element forming results are shown in Fig. 10a and b, respectively. The laboratory-formed part developed wrinkling at the front, back, and sides of the hemisphere (i.e., along the central axes of the planar

sheet but near the bottom of the 3-D part). The finite element analysis was also able to capture the development of these out-of-plane defects in these locations. The material draw-in is also observed to be well correlated between the experiament and the model. Overall, the initial modeling efforts show promise and good correlation with the wrinkles developed in the physical part during the forming trial. This excellent correlation between the model and the experiment implies that the model shows promise as a tool to design the size and shapes of the blanks to be used in the maufacturing process such that a near-net-shape preform can be achieved without wrinkling. The research for a future paper on the sensitivity of the formed part to the charge in the shape of the blanks comprising a helmet formulation is currently underway.

While good agreement can be seen upon visual inspection between the experimental and numerical preform shapes, i.e. location and shape of the out-of-plane waves, in Fig. 10, additional work is recommended to further validate the methodology shared in this paper for characterizing the bending rigidity. Currently, there is no standard test procedure for the measurement of the elevated-temperature flexural rigidity of fibrous composite prepregs. It is recommended that a benchmark study be conducted to compare the various available techniques.

Conclusions

This paper discussed approaches used to characterize the tensile and flexural behavior of Dyneema® HB80 at typical forming temperatures. These elevated-temperature data have not been documented in the open literature before now. Due to the low coefficient of friction, slipping of the sample in tension posed a problem to the collection of good experimental data. To address this issue, modified gripping of the specimens was implemented, and a large gauge length was used to mitigate the influence of slippage in the measurement. A new design for an elevated-temperature test fixture to measure the bending stiffness of the lamina was presented. The material constants derived from experiment were implemented into

Fig. 10 Dyneema® HB80 sheet formed at 100°C (**a**) experimentally and (**b**) virtually via FEA

(a)   (b)
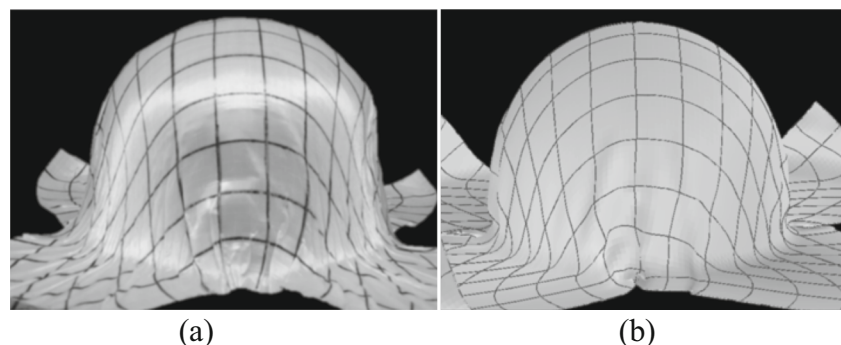
a discrete mesoscopic finite element model. A forming simulation was performed using this modeling technique, and the analysis results were assessed against a laboratory-formed part. The combination of tensile and flexural rigidities allowed out-of-plane defects to be captured in the model. Although good agreement was seen between experimental and numerical preform shapes upon visual inspection, indicating valid input data (e.g., bending stiffness), additional work is recommended to validate the method. Because no standard test procedure currently exists for measurement of elevated-temperature flexural rigidity of fibrous composite prepregs, a benchmark study is recommended in the future to compare the available techniques.

References

1. Majumdar S (2012) Growth opportunities: materials innovation will drive composites usage to new heights. High Perform Compos
2. Hallett SR, Jones MI, Wisnom, MR. (2013) Tension and compression testing of multi-directional laminates with artificial out of plane wrinkling defects. CompTest 2013-Book of Abstracts. :59
3. Borouchaki H, Cherouat A (2003) Geometrical draping of composite fabrics. Comptes Rendus Mecanique 331(6):437–442
4. Golden K, Rogers T, Spencer A (1991) Forming kinematics of continuous fibre reinforced laminates. Compos Manuf 2(3):267–277
5. Mack C, Taylor H (1956) 39—the fitting of woven cloth to surfaces. J Text Inst Trans 47(9):T477–TT88
6. Trochu F, Hammami A, Benoit Y (1996) Prediction of fibre orientation and net shape definition of complex composite parts. Compos A: Appl Sci Manuf 27(4):319–328
7. Jauffrès D, Sherwood JA, Morris CD, Chen J (2010) Discrete mesoscopic modeling for the simulation of woven-fabric reinforcement forming. Int J Mater Form 3(2):1205–1216
8. Bergsma OK (1995) Three dimensional simulation of fabric draping: TU Delft. Delft University of Technology
9. Potter K, Khan B, Wisnom M, Bell T, Stevens J (2008) Variability, fibre waviness and misalignment in the determination of the properties of composite materials and structures. Compos A: Appl Sci Manuf 39(9):1343–1354
10. Syerko E, Comas-Cardona S, Binetruy C (2012) Models of mechanical properties/behavior of dry fibrous materials at various scales in bending and tension: a review. Compos A: Appl Sci Manuf 43(8):1365–1388
11. Vidal-Salle E, Boisse P (2009) Modelling the structures and properties of woven fabrics. Model Predicting Text Behav:144
12. Harrison P, Gomes R, Curado-Correia N (2013) Press forming a 0/90 cross-ply advanced thermoplastic composite using the double-dome benchmark geometry. Compos A: Appl Sci Manuf 54:56–69
13. Potter K (2002) Bias extension measurements on cross-plied unidirectional prepreg. Compos A: Appl Sci Manuf 33(1):63–73
14. Chen J, Niezrecki C, Sherwood J, Avitabile P, Rumsey M, Hughes S, et al. (2012) Effect of manufacturing-induced defects on reliability of composite wind turbine blades. Executive Summary Report #S51900000011598. <http://www.uml.edu/docs/DOE_DE-EE0001374_ProjectSummary_tcm18-139832.pdf> U.S. Department of Energy Award No. DE-EE0001374 ARRA Funding
15. Jauffrès D, Morris CD, Sherwood JA, Chen J (2009) Simulation of the thermostamping of woven composites: mesoscopic modelling using explicit FEA codes. Int J Mater Form 2(1):173–176
16. Petrov A (2013) Characterization and finite element modeling of unidirectional and stitched non-crimp double bias fabrics for manufacturing of composites with embedded cabling [Masters Thesis]: University of Massachusetts Lowell
17. Abaqus I (2005) Abaqus/explicit: advanced topics - abaqus/explicit vs. abaqus/standard. <http://imechanica.org/files/0-overview%20Explicit.pdf>
18. ASTM International (2012) Standard test method for stiffness of fabrics. www.astm.org2012
19. Dangora LM, Mitchell CJ, Sherwood JA (2015) Predictive model for the detection of out-of-plane defects formed during textile-composite manufacture. Compos A: Appl Sci Manuf 78:102–112
20. ASTM International (2010) Standard test method for tensile properties of yarns by the single-strand method. www.astm.org2010
21. ASTM International (2010) Standard test method for breaking force and elongation of textile fabrics (strip method). www.astm.org2010
22. Cao J, Akkerman R, Boisse P, Chen J, Cheng HS, de Graaf EF et al (2008) Characterization of mechanical behavior of woven fabrics: experimental methods and benchmark results. Compos A 39:1037–1053
23. McGuinness G, Canavan R, Nestor T, O'Bradaigh C (1995) A picture-frame intraply shearing test for sheet-forming of composite materials. Proc ASME Mater Div, MD 39(2):1107–1118
24. Wang J, Page J, Paton R (1998) Experimental investigation of the draping properties of reinforcement fabrics. Compos Sci Technol 58(2):229–237
25. Dangora LM, Hansen CJ, Mitchell CJ, Sherwood JA, Parker JC (2015) Challenges associated with shear characterization of a cross-ply thermoplastic lamina using picture frame tests. Compos A: Appl Sci Manuf 78:181–190
26. Sachs U, Fetfatsidis KA, Schumacher J, Ziegmann G, Allaoui S, Hivet G, et al. (2012) A friction-test benchmark with Twintex PP. Key engineering materials: Trans Tech Publ; . p. 307–312
27. Chocron S, Nicholls AE, Brill A, Malka A, Namir T, Havazelet D et al (2014) Modeling unidirectional composites by bundling fibers into strips with experimental determination of shear and compression properties at high pressures. Compos Sci Technol 101:32–40
28. Hudspeth M, Nie X, Chen W (2012) Dynamic failure of Dyneema SK76 single fibers under biaxial shear/tension. Polymer 53(24):5568–5574
29. Heisserer U (2011) Tensile properties of Dyneema® HB plies (HB2, HB26, HB50, HB80). Technical report, DSM-Dyneema
30. Defoirdt N, Biswas S, De Vriese L, Van Acker J, Ahsan Q, Gorbatikh L et al (2010) Assessment of the tensile properties of coir, bamboo and jute fibre. Compos A: Appl Sci Manuf 41(5):588–595
31. Joffe R, Andersons J, Wallström L (2003) Strength and adhesion characteristics of elementary flax fibres with different surface treatments. Compos A: Appl Sci Manuf 34(7):603–612
32. Sekine N, Takao T, Shoji T, Toyama H, Kashiwazaki K, Sugasawa N et al (2001) Frictional coefficients of structural materials in AC superconducting coils. Cryogenics 41(5):379–384
33. Alger MS (1997) Polymer science dictionary: springer science & business media
34. Afshari M, Sikkema DJ, Lee K, Bogle M (2008) High performance fibers based on rigid and flexible polymers. Polym Rev 48(2):230–274
35. Lammens N, Kersemans M, Luyckx G, Van Paepegem W, Degrieck J (2014) Improved accuracy in the determination of

flexural rigidity of textile fabrics by the Peirce cantilever test (ASTM D1388). Text Res J 0040517514523182

36. Liang B, Hamila N, Peillon M, Boisse P (2014) Analysis of thermoplastic prepreg bending stiffness during manufacturing and of its influence on wrinkling simulations. Compos A: Appl Sci Manuf 67:111–122

37. Margossian A, Ding M, Avila Gray L, Bel S, Hinterhölzl R. (2014) Flexural characterisation of unidirectional thermoplastic tapes using a dynamic mechanical analysis system. Proceedings of the 16th European Conference on Composite Materials (ECCM16)2014

38. Sachs U, Akkerman R, Haanappel SP (2014) Bending Characterization of UD Composites. Key Eng Mater 611-612: 399–406

39. Martin T, Mander S, Dykes R, Bhattacharyya D (1997) Bending of continuous fibre-reinforced thermoplastic sheets. Compos Mater Ser 11:371–401

40. Dangora LM, Mitchell, CJ, Sherwood, JA, Parker JC (2016) Deepdraw forming trials on a cross-ply thermoplastic lamina for helmet preform manufacture. J Manuf Sci Eng 139(3):031009-031009-8. doi:10.1115/1.4034791